Clays and Clay Minerals, Vol. 54, No. 1, 45–53, 2006.

Eu(III) COPRECIPITATION WITH THE TRIOCTAHEDRAL CLAY MINERAL, HECTORITE

HEIKE PIEPER*, DIRK BOSBACH, PETRA J. PANAK, THOMAS RABUNG AND THOMAS FANGHÄNEL

Forschungszentrum Karlsruhe, Institut für Nukleare Entsorgung (INE), PO Box 3640, 76021 Karlsruhe, Germany

Abstract—Various secondary phases formed during alteration/dissolution of HLW (high-level nuclear waste) borosilicate glass represent a significant retention potential for radionuclides including trivalent actinides. The trioctahedral smectite, hectorite, $Na_{0.7}[Li_{0.7}Mg_{5.3}Si_8O_{20}(OH)_4]$, is one of the secondary phases identified within the alteration layer of corroded HLW glass. Numerous studies have clearly shown that many radionuclides are associated with clay minerals and the migration of radionuclides is strongly reduced by complexation. Due to the structural complexity and chemical variability of smectites, sorption of radionuclides involves several sorption mechanisms: (1) adsorption via inner-sphere and outer-sphere complexation; (2) cation exchange in the interlayer; and (3) incorporation into the smectite structure. Up to now, it was not known whether trivalent actinides such as Cm(III) and Am(III) become incorporated into the crystal structure of clay minerals like hectorite. We have used a new method, developed by Carrado *et al*. (1997b), to synthesize a Eu- and a Cm-containing hectorite, utilizing Cm(III) and chemically homologous Eu(III) coprecipitated with $Mg(OH)_2$ as a precursor. X-ray diffraction, Fourier transform infrared spectroscopy and atomic force microscopy identified the reaction products unambiguously as hectorite. The sorption mechanisms of Eu associated with the synthesized hectorite were investigated by time-resolved laser fluorescence spectroscopy (TRLFS). An unhydrated Eu species (fluorescence lifetime 930 μs) and a partly hydrated Eu species (fluorescence lifetime 381 μs) could be identified. The unhydrated Eu species can be interpreted as incorporating Eu(III) into the hectorite structure or a remaining X-ray amorphous silica phase. The spectra of Eu hectorite and the Eu silica complexation are too similar to permit differentiation between these species, but dialysis experiments demonstrated the close association of the unhydrated Eu species with the crystalline hectorite phase. Time-resolved laser fluorescence spectroscopy (TRLFS) measurements identified the same incorporated Eu species as long as the Eu hectorite was stable under acidic conditions. The stability of the Eu hectorite could be shown by the dialysis experiment over a time period of 160 h. Between 160 und 500 h, hectorite became unstable and a new silica phase was detected. In addition, TRLFS measurements of the Cm-containing hectorite confirmed the incorporation of actinides in the smectite structure. The Cm-hectorite and Cm-silica species can be differentiated unambiguously by TRLFS. In order to differentiate between coprecipitated and surface-sorbed Eu species, batch sorption studies were performed with synthetic Eu-free hectorite. For the surface-sorbed Eu species, a fluorescence lifetime of 284 μs (3.1 H_2O molecules) was found, which clearly differs from the coprecipitated species with a fluorescence lifetime of 930 μs. The different lifetimes indicate a different chemical environment. Based on all observations it seems to be very likely that trace amounts of Cm/Eu occupy a distorted octahedral site in the hectorite.

Key Words—Actinides, Coprecipitation, Curium (Cm), Europium (Eu), High-level Nuclear Waste Glass (HLW) Corrosion, Lanthanides, Lattice Substitution, Organo-hectorite, Smectite, Time-resolved Laser Fluorescence Spectroscopy (TRLFS).

INTRODUCTION

Clay-based materials are known to be efficient geotechnical barriers for disposal of nuclear waste within deep geological formations (Mallants *et al*., 2001; Meunier *et al*., 1998; Rochelle *et al*., 1996). Numerous studies have demonstrated that radionuclides tend to sorb on clay minerals *via* various reaction mechanisms. Trivalent actinides, in particular, are known to be adsorbed on smectite-like minerals by outer- and inner-sphere surface complexes, retarding the migration of radionuclides into the environment. Outer-sphere complexation dominates the sorption process in the lower pH range (<4), while at higher pH, inner-sphere complexation prevails (Stumpf *et al.*, 2002; Coppin *et al.*, 2002; Stumpf *et al.*, 2001; Malakul *et al.*, 1998; Maza-Rodriguez *et al.*, 1992; Miller *et al.*, 1983, 1982). These studies have focused on radionuclide adsorption to pre-existing clay minerals. However, during the geochemical evolution of the waste matrix over geological timescales, the waste matrix may dissolve upon contact with groundwater. New secondary alteration phases may form, including clay minerals (Vidal *et al.*, 1995).

It is well known that trivalent actinides coprecipitate with various secondary phases, such as phosphates, sulfates and molybdates, which are formed during HLW

* E-mail address of corresponding author:
pieper@ine.fzk.de
DOI: 10.1346/CCMN.2006.0540106

glass or spent fuel corrosion. During coprecipitation, actinides can be incorporated into the structure of these secondary phases (Abdelouas *et al.*, 1995, 1996; Luckscheiter and Nesovic, 1996; Luckscheiter and Kienzler, 2001; Zimmer *et al.*, 2002; Bosbach *et al.*, 2002, 2004). The formation of clay minerals opens the possibility of incorporating actinides within the crystal structure of smectites. The isolation of single reaction steps from complex corrosion processes, like clay formation, requires synthesis under controlled conditions. Additionally, coprecipitation experiments involve laboratory synthesis of clay minerals. Unfortunately, reaction kinetics for the formation of most clay minerals are extremely slow (Velde, 1995), which implies time-consuming and complex experiments. Use of organic additives offers an opportunity to avoid these kinetic problems (Carrado, 2000).

In this study, we focused on the synthesis of organo-hectorite ($Na_{0.7}[Li_{0.7}Mg_{5.3}Si_8O_{20}(OH)_4]$) and the coprecipitation with either Cm(III) or Eu(III) as a nonradioactive chemical homologue for trivalent actinides (Chapman and Smellie, 1986). Hectorite has been identified in long-term corrosion experiments as one of the secondary phases forming in the alteration layer of HLW glass under near-field conditions (Zwicky *et al.*, 1989).

We have used a novel method to synthesize hectorite nanoparticles at $\leqslant$100ºC within 48 h by using an organic additive (Carrado *et al.*, 1997b). Hectorite is composed of one sheet of edge-sharing [Mg/LiO_6] octahedra sandwiched between two sheets of corner-sharing [SiO_4] tetrahedra. All octahedral sites are occupied with either Mg or Li. The unshared tetrahedra apices point in the direction of the octahedral sheet and connect the three sheets to the common *TOT* structure of 2:1 sheet silicates. The organic additive is situated in the interlayer between these *TOT* layers.

In nature, cation substitution is observed in the tetrahedral and octahedral sheets of smectites. Considering the ionic radii (Shannon and Prewitt, 1969) of the cations occupying regular lattice sites in the *TOT* structure of hectorite (^{IV}Si = 0.26 Å, ^{VI}Mg = 0.72 Å and ^{VI}Li = 0.76 Å) and the ionic radii of Cm(III) and Eu(III) (^{VI}Cm = 0.97 Å, ^{VI}Eu = 0.95 Å), it seems unreasonable to assume tetrahedral cation substitution. Incorporation of actinides and lanthanides presumably occur at octahedral sites in the hectorite structure. Laser fluorescence spectroscopy has been used to characterize the Cm and Eu species associated with the synthesized organo-hectorite.

EXPERIMENTAL

Synthesis and sample preparation

Freshly precipitated Mg hydroxide slurry was added to a 12 mmol/L lithium fluoride/4 mmol/L tetraethylammoniumchloride (TEA) solution. The suspension was stirred in a refluxed glass vessel. After 20 min, 72 mmol/L Ludox HS-30, a Na^+-stabilized 30% silica sol (Sigma-Aldrich), was added (Carrado *et al.*, 1997b, 2000). The syntheses were carried out at pH 9–10 and 100ºC (sample name: Hec) as well as 60ºC. All fresh reaction products were washed with HCl (ultrapure, Merck) at pH 3 to remove the remaining Mg hydroxide. In the coprecipitation experiments a Mg/Eu ratio of 100 was adjusted in the Mg/Eu-solution ($MgCl_2{\cdot}6H_2O$/$Eu(NO_3)_3{\cdot}6H_2O$) according to 24 mmol/L Mg (sample name: HecEu). A Eu solution was also added to Ludox HS-30 corresponding to the Si/Eu ratio and pH of the coprecipitation experiments and heated to 100ºC to obtain a reference spectrum of the Eu species.

40 mL of the decanted HecEu-suspension were placed in a dialysis membrane for up to 3 weeks (knotted Spectra/Por® 3 tube; molecular weight cut off: 3500 Dalton) in order to dissolve excess Ludox SiO_2 sol at pH 3 and room temperature and study the stability of the Eu hectorite. The dialysis tube with the trapped HecEu was placed in a 1 L PE-bottle filled with 10^{-3} mol/L HCl solution. Sedimentation was avoided by mixing continuously (Bibby Sterin, Roller Mixer SRT2). A small sample of the reacted solid was taken after 160 and 500 h of dialysis (HecEuDia1: 160 h, HecEuDia2: 500 h). The acidic solution was replaced at regular intervals (24 h). The Si concentration of the solution was measured as β-Silicomolybdenum blue with the Spectroquant® Si-test (Merck 1.14794). The potential precipitation of secondary phases other than hectorite during this procedure was excluded on the basis of geochemical calculations using PHREEQC (Parkhurst and Appelo, 1999; Nagra/PSI thermodynamic database, Hummel *et al.*, 2002).

Hectorite characterization

Sample characterization was performed using X-ray diffraction (XRD, Bruker D8 advanced, CuKα) with textured samples (Moore and Reynolds, 1997), photonc correlation spectroscopy (PCS, ZetaPlus, Brookhaven Inc., equipped with a 50 mW solid-state laser λ = 532 nm) and Fourier transform infrared (FTIR) spectroscopy (Bruker IFS 55). The FTIR spectra were recorded within the range 360–4000 cm^{-1}, collecting 256 scans at a resolution of 2 cm^{-1}. The pressed pellets contained 1 mg of material in 100 mg of dried KBr. The measurement chamber was first flushed for 20–30 min with N_2 gas to avoid carbon dioxide interference. Furthermore, the samples were characterized by scanning electron microscopy (SEM, Camscan 44FE) and atomic force microscopy (AFM, Veeco Instruments DIMENSION 3100 with Nanoscope IV controller and Topometrix, Explorer True Metrix). For SEM studies the Eu-free samples were sputtered with Cr (Edwards, Xenonsput), while Eu-containing samples were coated with C (Leybold-Heraeus, UNIVEX 300).

Atomic force microscopy was used to observe the heterogeneous hectorite nucleation *in situ* on a

https://doi.org/10.1346/CCMN.2006.0540106 Published online by Cambridge University Press

nanometer scale. The experiments were performed at room temperature. Freshly cleaved single mica crystals, $2.5 \times 1.0 \times \sim 0.02$ cm were each added to 20 mL of the synthesis suspension ($Mg(OH)_2$ slurry, LiF, Ludox HS-30, NO organic TEA additive) as an atomically flat substrate (Plano GmbH, Germany). Sedimentation was avoided by mixing continuously (Bibby Sterin, Roller Mixer SRT2). The mica was chosen because its *TOT* structure matches that of hectorite. After 2 and 8 weeks, a mica substrate was washed with Milli-Q water to remove loose components of the suspension and measured in AFM contact mode while still exposed to the aqueous solution. Contact mode was used to identify possible extant loose particles. Such loose particles move during the scan and generate characteristic artifacts, in contrast to the grown hectorite particles. Substrates were also exposed to the pure precursor suspension and to a mixture of the other components (LiF and Ludox HS-30) for reference.

Speciation of the Cm or Eu ions associated with the hectorite phase

The synthesis procedure for Eu-hectorite had to be modified to accomplish Cm coprecipitation with $Mg(OH)_2$, due to the limited availability of Cm-248. One batch contains 5 mL of Cm hectorite starting suspension in contrast to the Eu-containing synthesis with 500 mL. 50 µL of the 2.11×10^{-5} mol/L Cm stock solution were coprecipitated with $Mg(OH)_2$ at a Mg/Cm ratio of 227500. Curium stock solution was also added to Ludox HS-30 corresponding to the Si/Cm ratio of the coprecipitation experiments to obtain a reference spectrum of the Cm species associated with silica under the same conditions. The glass vessels were locked with caps used for autoclaving. These vessels were placed in a drying cabinet at 90ºC for 3 days and an external magnetic stirrer was used to avoid sedimentation. The Cm stock solution consists of 89.68% Cm-248, 0.07% Cm-247, 9.38% Cm-246, 0.14% Cm-245, 0.30% Cm-244 and 0.43% Cm-243 in 1.0 mol/L $HClO_4$.

Time-resolved laser fluorescence spectroscopy (TRLFS) measurements were performed with an excimer pumped dye laser system (Lamda Physics, EMG 201 and FL 3002) at a constant excitation wavelength of 394.0 nm for Eu(III) and 375.0 nm for Cm(III). Emission spectra were recorded from 580 to 620 nm using a delay time of 1.2 µs at a gate width of 1.3 ms by an optical multichannel analyser, which consists of a polychromator (Jobin Yvon, HR 320) with a 1200 lines/mm grating and a time-gateable photodiode array with 1024 Si photo diodes (Spectroscopy Instruments, ST 180, IRY 700 G). Details of the spectroscopic set-up are given elsewhere (Chung *et al.*, 1998).

All measured samples contain 300 µL of hectorite suspension added to 2.5 mL of MilliQ-water or Eu solution in the adsorption experiments.

RESULTS AND DISCUSSION

Four different sample types were studied in detail: (1) HCl-washed, Eu-free sample 'Hec'; (2) HCl-washed, Eu-containing sample 'HecEu'; (3) solid-phase sample remaining after 160 h of dialysis 'HecEuDia1', the period of time to reach a constant Si release (5±0.5 ppm/day); and (4) the long-term leaching sample after 500 h of dialysis 'HecEuDia2'. All these samples were synthesized at 100ºC.

Hectorite characterization

X-ray diffraction. The XRD measurements of the Eu-free hectorite samples synthesized at 100 and 60ºC indicated a basal spacing of 14.3–14.5±0.3 Å, which is a typical *d* spacing for organo-hectorite with tetraethylammonium ions in the clay interlayer (Carrado, 2000). Unfortunately, higher 00l reflections could not be identified. A comparable XRD pattern with a basal spacing of 14.5±0.3 Å was observed for the Eu-containing sample HecEu (100ºC) (Figure 1). Considering the difference in ionic radii of Eu(III) and Mg(II) (Shannon and Prewitt, 1969) and the error in *d* spacing, an influence of the coprecipitated Eu(III) on the XRD pattern could not be observed. Additionally, the amount of Eu substitution is too small to have an effect on the *d* spacing.

FTIR spectroscopy. The FTIR spectroscopy clearly showed that the synthesized samples Hec and HecEu are hectorite with the characteristic OH-stretching band of the Mg_3OH unit at 3681 cm^{-1} and its OH-deformation band at 657 cm^{-1} combined with the absorption bands of the Si–O units at 1024 and 470 cm^{-1} (Figure 1b) (Farmer, 1974; Madejová and Komadel, 2001). All remaining absorption bands of the products correspond to IR spectra of organo-hectorite (Carrado *et al.*, 1997a). An additional absorption band at 799 cm^{-1} is related to X-ray amorphous silica indicating the presence of unreacted Ludox HS-30 or reprecipitated X-ray amorphous silica (Farmer, 1974). None of the Eu-containing samples showed the characteristic $Eu(OH)_3$ absorption band at 3605 cm^{-1} (Farmer, 1974).

Scanning electron microscopy. The SEM images of the different hectorite samples synthesized at 100ºC (Hec, HecEu and HecEuDia1, Figure 2b–d) showed irregularly shaped platy crystals, which have been described as "a corn-flake-like morphology" (Moore and Reynolds, 1997). Such crystal morphology is typical for natural minerals formed at high precipitation rates (Sunagawa, 1987). A significant variation in the particle morphology as a function of Eu content or dialysis time was not observed.

In contrast, SEM images of Eu-free hectorite samples synthesized at different temperatures indicate a strong temperature dependency of the crystal morphology and particle size. The crystals synthesized at 60ºC are

https://doi.org/10.1346/CCMN.2006.0540106 Published online by Cambridge University Press

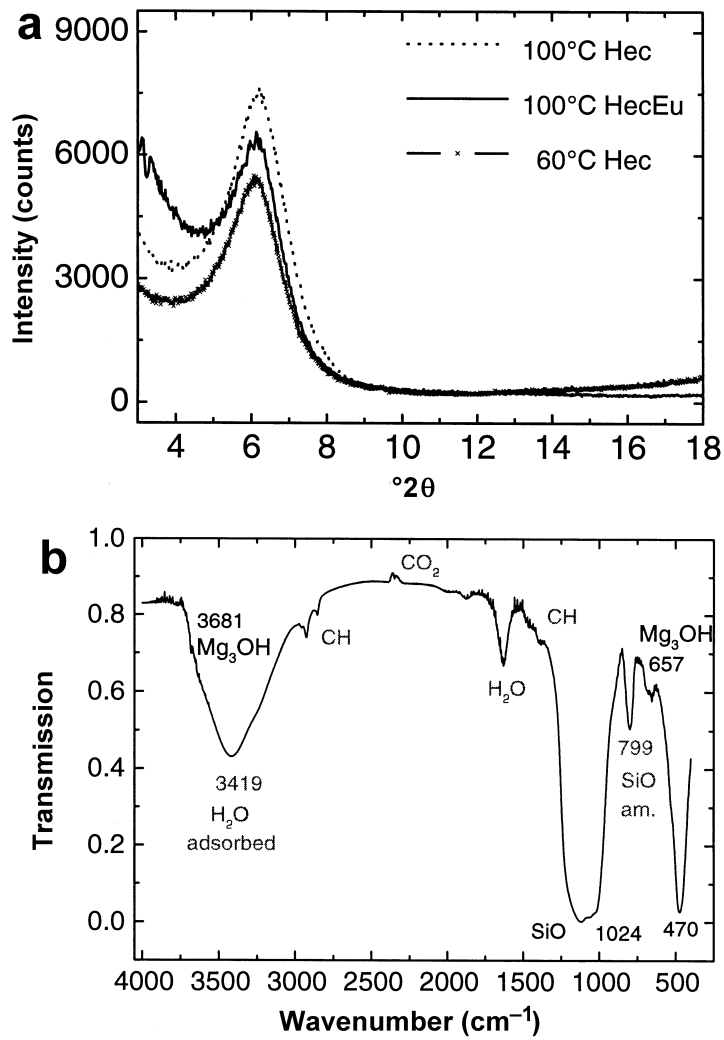

Figure 1. (a) X-ray powder diffraction (CuKα, oriented aggregates on a glass slide). The 001 basal reflection of hectorite synthesized at 100ºC (···, uppermost) and 60ºC (x−x−x, lowermost) showed typical *d* spacings of organo-hectorite with TEA in the clay interlayer. The incorporation of trace amounts of Eu(III) into the octahedral sheet did not change the *d* spacing, as shown in the pattern of the Eu-containing sample HecEu, synthesized at 100ºC (——, middle). (b) FTIR spectroscopy. The IR spectrum identified the precipitated sample HecEu as organo-hectorite.

dominated by the energetically favored (00l)-basal face and the (*hk*0)- and (0*k*0)-edge crystal faces (Figure 2a; Bosbach *et al.*, 2000, Bickmore *et al.*, 2001). The flat crystal morphology with well defined crystallographic edge faces corresponds to the predicted crystal morphology based on periodic bond-chain theory (Hartman, 1987). A temperature dependency of the particle size was also observed by photon correlation spectroscopy. The average size of the particles formed at 100ºC is ~650 nm, while the particles formed at 60ºC have an average size of 290 nm. This indicates an increased crystal growth rate with increasing temperature related to the formation of kink-sites on the clay surfaces. The coprecipitation of small amounts of Eu(III) will have a negligible effect on the temperature dependency, as mentioned above.

HETEROGENEOUS NUCLEATION

The heterogeneous formation of nano-scale hectorite nuclei on a mica 001 substrate (without the additive TEA) was observed with AFM. The nuclei detected after two weeks (Figure 3a) had a platy morphology with an average height of 13±2 Å, corresponding to literature data of one hydrated *TOT* layer of hectorite (Güven, 1988). Hectorite particles continued to grow for another 6 weeks and developed to disc-like particles (Figure 3b) with heights of up to 42±5 Å, representing up to three *TOT* layers. From the temporal change of the particle dimensions without TEA, a surface area-normalized crystal growth rate of 3×10^{-12} mol m^{-2} s^{-1} was determined. Loose particles were not observed.

This experiment was also carried out with an Eu-containing precursor. Atomic force microscopy measure-

https://doi.org/10.1346/CCMN.2006.0540106 Published online by Cambridge University Press

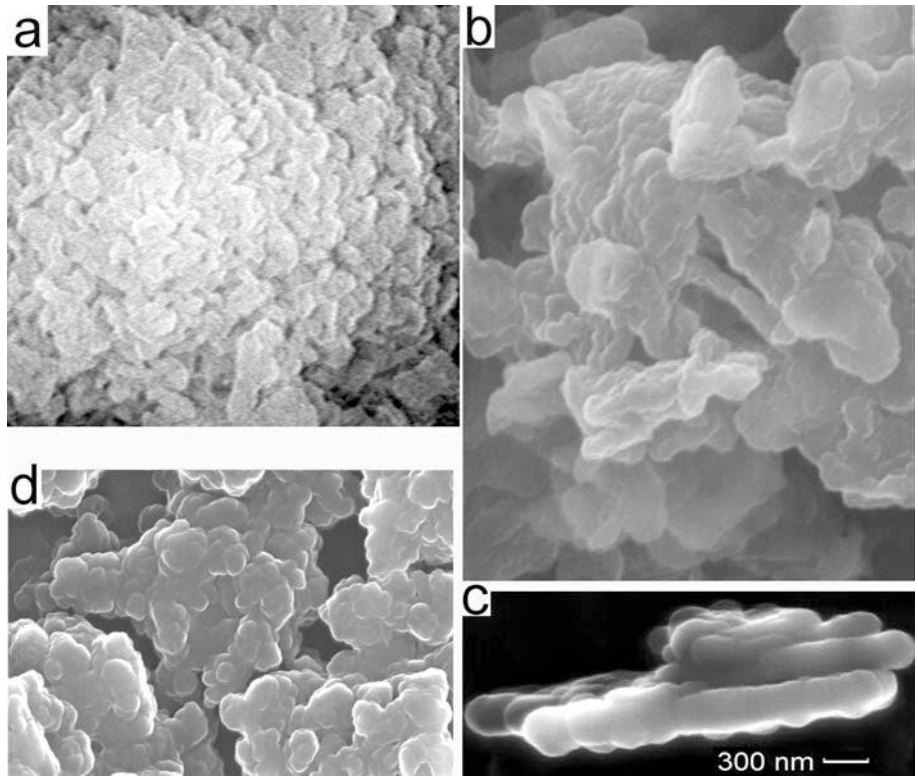

Figure 2. Scanning electron microscopy (accelerating voltage: 25 kV; I = 0.5 mA). (a) Eu-free particles synthesized at 60ºC were dominated by the energetically favored (001) basal face and the (hk0) and (0k0) crystal faces. Image 6 μm wide. (b) Eu-free particles synthesized at 100ºC (Hec) were irregularly shaped platy crystals. Image is 3 μm wide. (c) Eu-containing particles, synthesized at 100ºC (HecEu), appeared the same as Hec. Some of the particles were lath-like as observed in natural hectorite samples (Bosbach *et al.*, 2000). (d) Eu-containing particles after 160 h of dialysis (HecEuDia1) appear the same as the original sample, HecEu. Image is 10 μm wide.

ments showed that the nuclei were built similar to the nuclei of the Eu-free experiment, but the stacking of more than one *TOT* layer appeared to be inhibited.

DIALYSIS

In order to purify the hectorite reaction product from unreacted Ludox and to study the long-term stability of the Eu-hectorite, HecEu was dialyzed at pH 3. The remaining Ludox X-ray amorphous silica phase was expected to be removed by preferential dissolution in a dialysis membrane, due to the greater dissolution rate of X-ray amorphous silica/Ludox compared to the dissolution rate of hectorite. After 160 h of treatment, FTIR measurements identified the solid phase as hectorite, but after 500 h of treatment, complete dissolution of the crystalline hectorite was observed. The FTIR spectrum of HecEuDia2 shows, in contrast to Hec, HecEu and HecEuDia1, no Mg bands and it exhibits an additional absorption band at 968 cm^{-1} (Figure 4). This new absorption band is a common feature of impurities in a silica phase or an indication of hydrous silica ($SiO_2 \times nH_2O$); (Farmer, 1974). It would appear that a new silica phase formed during the late-stage hectorite dialysis, probably as an alteration product of hectorite. The TRLFS clearly showed that no Eu is associated (adsorbed/incorporated) with this X-ray amorphous residue from HecEuDia2, in contrast to the untreated product HecEu and the HecEuDia1 sample dialyzed for 160 h. Based on these data we can conclude that Eu(III) is closely associated with the crystalline hectorite.

The sorption mechanisms of the trivalent f-elements Eu and Cm

Speciation of the Eu ions associated with the hectorite phase. Due to the compositional variability and structural complexity of smectite-like minerals, verification of Eu(III) incorporation into the *TOT* structure is difficult. Therefore, TRLFS was used to characterize the Cm or Eu species associated with the hectorite phase. The Eu fluorescence emission bands $^5D_0 \rightarrow {}^7F_1$ and $^5D_0 \rightarrow {}^7F_2$ show no significant peak shift upon changing the chemical environment of the Eu species. Hence, the peak position of Eu fluorescence emission bands gave no information about the species, but the intensity of the $^5D_0 \rightarrow {}^7F_x$ transitions and the fine structure of the emission bands change significantly when an Eu-aquo ion interacts with a mineral surface or is incorporated in

https://doi.org/10.1346/CCMN.2006.0540106 Published online by Cambridge University Press

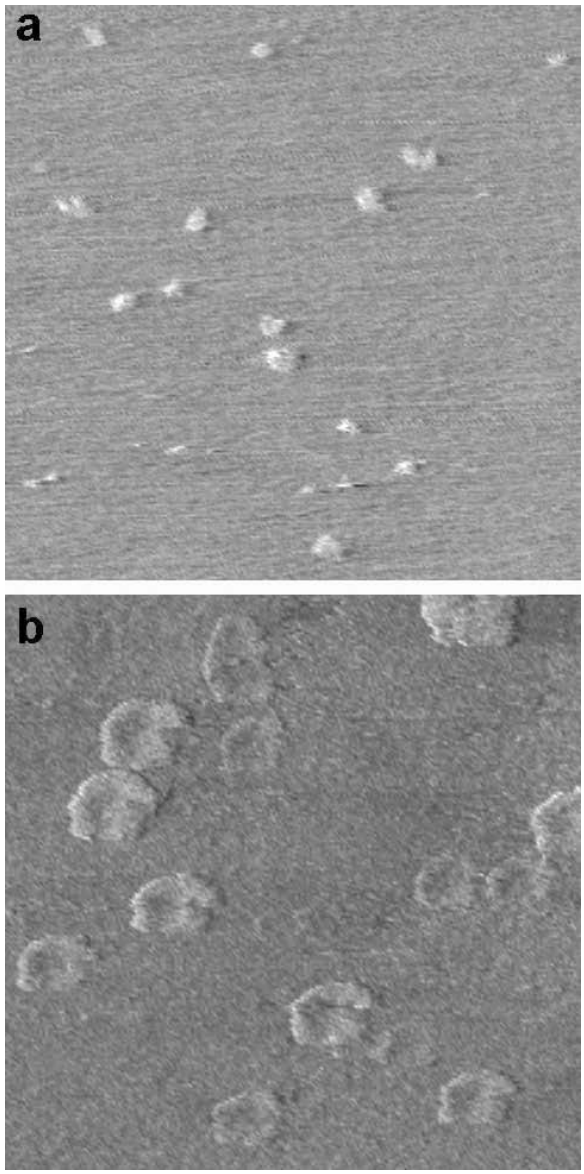

Figure 3. Heterogeneous nucleation at room temperature without organic additive (atomic force microscopy, contact mode). (a) After 2 weeks: heterogeneous formation of hectorite nuclei on a mica substrate. The particle height represented is one *TOT* layer. Image is 530 nm wide. (b) After 8 weeks: the nuclei grew to disc-like particles of three *TOT* layers. Image is 370 nm wide.

the mineral structure. This dependency of the emission band intensities on the first coordination sphere is a consequence of the hypersensitive effect (Bünzli and Choppin, 1989).

In contrast to the Eu-aquo species, the Eu emission spectrum of Eu-hectorite (HecEu as well as HecEuDia1) shows a weak emission band of the $^5D_0 \rightarrow {}^7F_1$ transition and a strong emission band of $^5D_0 \rightarrow {}^7F_2$ transition (Figure 5). In particular, the splitting of the $^5D_0 \rightarrow {}^7F_2$ peak indicates a strong ligand field effect (Figure 5). Plotting the intensity of the $^5D_0 \rightarrow {}^7F_1$ and $^5D_0 \rightarrow {}^7F_2$

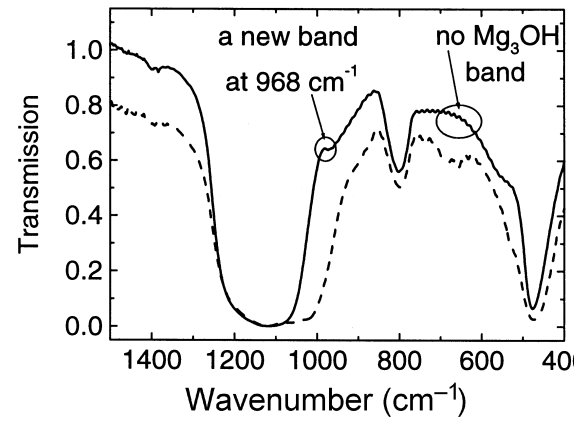

Figure 4. FTIR spectroscopy. (- - -) Eu-containing hectorite after 160 h of dialysis, HecEuDia1. No difference compared to the unleached sample HecEu (Figure 1b). (——) FTIR spectrum of the long-term leached sample HecEuDia2 showed that the crystalline hectorite has been completely dissolved. An additional absorption band at 968 cm^{-1} indicates a new silica phase. No Eu(III) was associated with this X-ray amorphous residue.

emission as a function of the delay time allows us to determine the fluorescence lifetime of a species. The decay of the Eu hectorite fluorescence emission signal as a function of the delay time follows a bi-exponential function (Figure 6), indicating the presence of at least two Eu species. Empirical correlations between H_2O/OH^- ligands and the reciprocal fluorescence lifetime (*e.g.* $n_{H_2O(Eu)} = 1.07*K_{obs(Eu)} - 0.62$) were used to estimate the number of H_2O molecules in the inner coordination sphere of the two types of Eu species associated with the hectorite (Horrocks *et al.*, 1979; Kimura *et al.*, 1994). These estimates showed 2.8±1 H_2O molecules for the HecEuDia1 sample (315 μs lifetime) and 2.2±1 H_2O molecules for the HecEu sample (381 μs lifetime). The partly hydrated Eu species were not further considered, but the deviance in lifetimes can either denote an additional Eu species or a small change in the chemical environment. Both reasons for possible variances of the original sample can be explained by the dialysis process. Furthermore, a lifetime of 955 μs (930 μs in HecEu) indicates an Eu species which has lost its entire hydration sphere. Therefore, we ascribe the Eu species with the longer lifetime of 955 μs/930 μs (both 0.5±1 H_2O) to an unhydrated Eu ion incorporated in the *TOT* structure or in the minor X-ray amorphous silica phase remaining during the hectorite synthesis.

The silica/Eu(III) complexation was studied in detail with TRLFS (Takahashi *et al.*, 1998; Chung *et al.*, 1998), but in fact, the very similar spectra of Eu-hectorite and the Eu-silica species cannot be differentiated (see Figure 5). The fluorescence lifetimes of the Eu\Ludox system were determined as 348 and 779 μs. The 779 μs lifetime assigned to an incorporated Eu silica species is shorter than the incorporated Eu hectorite species, but Eu incorporation into the silica during the hectorite synthesis cannot be excluded.

https://doi.org/10.1346/CCMN.2006.0540106 Published online by Cambridge University Press

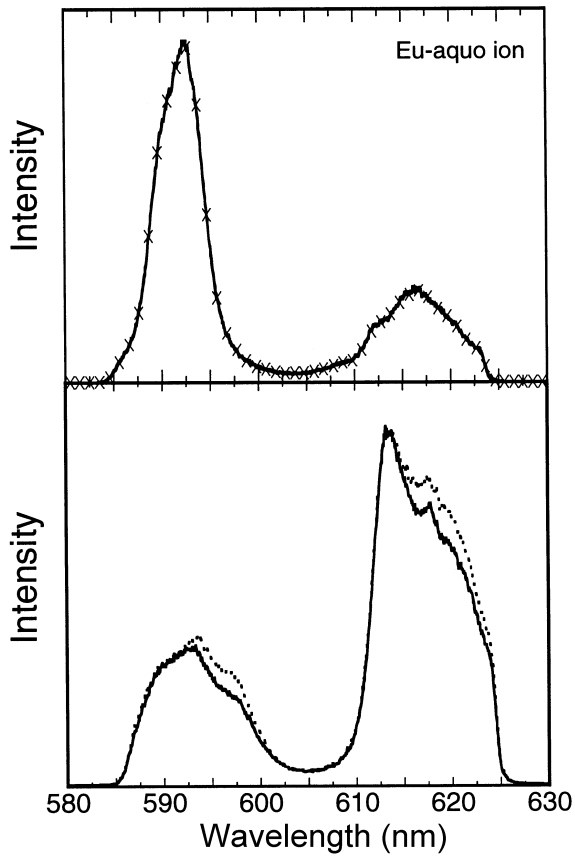

Figure 5. Time-resolved laser fluorescence spectroscopy. The emission spectrum of Eu-containing hectorite (HecEu, —) showed, in contrast to the Eu-aquo ion (x-x-x), a significant greater intensity of the $^5D_0 \rightarrow {}^7F_2$ transition than the $^5D_0 \rightarrow {}^7F_1$ transition. This reversal of the F_1/F_2-ratio indicated a change in the chemical environment. Additionally, the splitting of the $^5D_0 \rightarrow {}^7F_2$-peak indicated a strong complexation of the Eu(III) ion. The emission spectra of Eu-hectorite and the Eu-silica complexes (Ludox HS-30, heated for 3 days to 100ºC, - - -) were almost identical and cannot be differentiated.

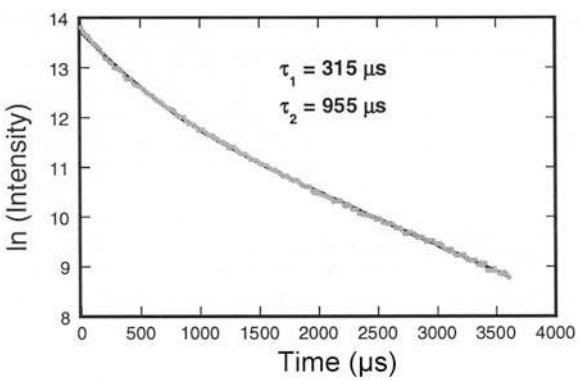

Figure 6. Time-resolved laser fluorescence spectroscopy. The fluorescence emission decay was observed to follow a bi-exponential function, according to at least two different species in the sample HecEuDia1. The lifetime of 315 µs corresponds to a species coordinated by 2–3 H_2O/OH^-. The lifetime of 955 µs indicates a Eu species which has lost almost its entire hydration sphere.

Speciation of the Cm(III) ions associated with the hectorite phase. In contrast to the emission bands of the Eu species, the Cm-fluorescence emission band $^6D_{7/2} \rightarrow {}^8S_{7/2}$ is affected by the chemical environment of the species. Hence, Cm-fluorescence spectroscopy provides more information, and coprecipitation experiments with Cm were performed in order to clarify which phase incorporates trivalent actinides (and lanthanides). The Cm hectorite shows a fluorescence band at 610 nm due to the $^6D_{7/2} \rightarrow {}^8S_{7/2}$ transition of Cm(III). A significant peak shift of ~16 nm compared to the peak position of the aquo ion at 593.8 nm is observed (Figure 7). The change of the chemical environment in the first coordination sphere of the Cm ion, accompanied by a loss of H_2O or OH^-, leads to a red shift of the emission band. Two Cm species, an adsorbed and an incorporated species, contribute to the fluorescence signal of the Cm hectorite. These two Cm species exhibit different fluorescence emission wavelengths. Therefore, the exact position and shape of the fluorescence emission band of Cm hectorite depends on the relative amount of these two species and can be influenced slightly by variation of the synthesis conditions.

In the emission reference spectrum of Cm associated with Ludox HS-30, we found an 11.3 nm red shift to 605.1 nm compared to the Cm-aquo ion. Due to the significant difference in peak position of >4 nm between the Cm-silica complex and the Cm hectorite species, we can differentiate unambiguously between these two species. As a result of the Cm experiment we can deduce that Eu/Cm must be incorporated into the hectorite structure.

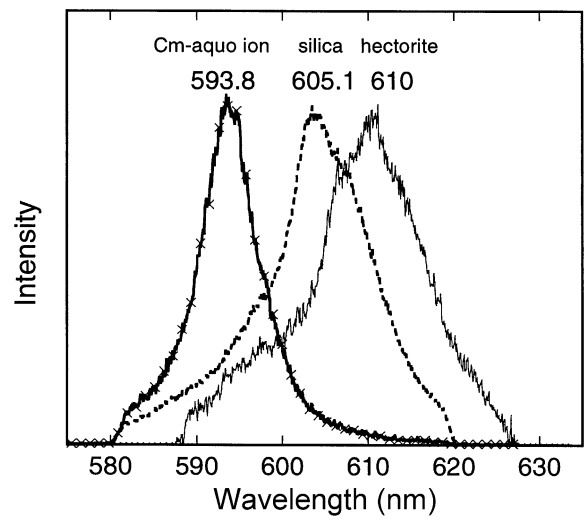

Figure 7. Cm(III)-time-resolved laser fluorescence spectroscopy. A fluorescence emission band of Cm-hectorite, synthesized at 90ºC (—, maximum at 610 nm, two species: adsorbed and incorporated) compared to the Cm-aquo ion (x-x-x, maximum at 593.7 nm, one species) and the Cm-silica (- - -, maximum at 605.1 nm, one species, Ludox-HS 30 heated up to 90ºC).

https://doi.org/10.1346/CCMN.2006.0540106 Published online by Cambridge University Press

Eu(III) ion interaction with pure hectorite and subsequent speciation

Batch type Eu(III) adsorption experiments onto synthetic Eu-free hectorite (Hec) were carried out at pH 6.5 at room temperature under ambient conditions. The ionic strength was not adjusted to obtain a reference spectrum of a Milli-Q-washed hectorite with Eu(III) still adsorbed. The TRLFS measurements show that sorption occurs at pH 6.5 almost instantaneously after adding Eu(III) solution ([Eu] = 10^{-4} mol/L and 10^{-6} mol/L) to the hectorite suspension. The fluorescence lifetime of 284 µs indicates ~3.1±1 water molecules in the first coordination sphere of the Eu species. The fluorescence lifetime is somewhat greater than found for the inner-sphere surface complex observed for Eu(III) sorption to natural Al-containing smectite under a CO_2-free atmosphere (188±20 µs, pH 7.16 Stumpf *et al.*, 2002). However, it is known that under aerobic conditions, ternary carbonate surface complexes may form and can be responsible for an increase of the fluorescence lifetime up to 333±20 µs at pH 7.11 (Stumpf *et al.*, 2002). Formation of such ternary surface complexes cannot be excluded at the experimental conditions applied in the present study. After reducing the pH of the batch adsorption experiment ([Eu] = 10^{-4} mol/L) from pH 6.5 to 4, desorption of the surface-sorbed Eu(III) species occurred instantaneously. In contrast, no significant release of Eu(III) was observed due to acidification of the HecEuDia1 sample to pH 4. The Eu spectra of the acidified sample HecEuDia1 (pH 4) and HecEuDia1 were found to be identical, which means that Eu species incorporated into the structure remained stable for some hours under acidic conditions. The long-term stability of Eu-containing hectorite was shown by the dialysis of HecEu. From TRLFS results it can be concluded that Eu(III) was incorporated into the hectorite samples before the dialysis and after 160 h of dialysis (HecEu, HecEuDia1).

CONCLUSIONS

We have synthesized a Eu(III)- and a Cm(III)-containing trioctahedral smectite-like mineral (hectorite). Combining macroscopic wet chemical techniques with laser fluorescence measurements clearly shows that unhydrated Eu(III) or Cm(III) species are closely associated with hectorite. The TRLFS measurements of the Cm-containing hectorite allow unambiguous differentiation between the Cm-silica species and the Cm species incorporated into the hectorite.

Considering the ionic radii of the cations Mg and Li (0.72 Å/0.76 Å) occupying octahedral sites in the *TOT* structure of hectorite and the ionic radii of ^{VI}Cm(III) and ^{VI}Eu(III) (0.97 Å/0.95 Å), it seems unreasonable to assume a simple cation substitution. However, our TRLFS data combined with a well controlled synthesis are clearly compatible with the assumption of Eu/Cm in an octahedral site. We expect to confirm this conclusion with an extended X-ray absorption fine structure study as measurements at the Eu(III) L3 edge will allow us to probe the local environment around the Eu cations in more detail.

REFERENCES

Abdelouas, A., Crovisier, J.L., Lutze, W., Muller, R. and Bernotat, W. (1995) Structure and chemical properties of surface layers developed on R7t7 simulated nuclear waste glass altered in brine at 190ºC. *European Journal of Mineralogy*, **7**, 1101–1113.

Abdelouas, A., Crovisier, J.L., Lutze, W., Grambow, B., Dran, J.C. and Müller, R. (1997) Surface layers on a borosilicate nuclear waste glass corroded in $MgCl_2$ solution. *Journal of Nuclear Materials*, **240**, 100–111.

Bickmore, B.R., Bosbach, D., Hochella, M.F., Charlet, L. and Rufe, E. (2001) In situ atomic force microscopy study of hectorite and nontronite dissolution: Implications for phyllosilicate edge surface structures and dissolution mechanisms. *American Mineralogist*, **86**, 411–423.

Bosbach, D., Charlet, L., Bickmore, B. and Hochella, M.F., Jr. (2000) The dissolution of hectorite: in-situ, real-time observations using atomic force. *American Mineralogist*, **85**, 1209–1216

Bosbach, D., Rabung, T. and Luckscheiter, B. (2002) Cm^{3+}/Eu^{3+} coprecipitation with powellite ($CaMoO_4$) during HLW glass corrosion. *Geochimica et Cosmochimica Acta*, **66**, A93–A93.

Bosbach, D., Rabung, T., Brandt, F. and Fanghaenel, T. (2004) Trivalent actinide coprecipitation with powellite (CaMoO4): Secondary solid solution formation during HLW borosilicate-glass dissolution. *Radiochimica Acta*, **92**, 639–643.

Bünzli J.-C.G. and Choppin, G.R. (editors) (1989) *Lanthanide Probes in Life, Chemical and Earth Sciences*. Elsevier, Amsterdam.

Carrado, K.A. (2000) Synthetic organo- and polymer-clays: preparation, characterization, and materials applications. *Applied Clay Science*, **17**, 1–23.

Carrado, K.A., Thiyagarajan, P. and Song, K. (1997a) A study of organo-hectorite clay crystallization. *Clay Minerals*, **32**, 29–40

Carrado, K.A., Zajac, G.W., Song, K. and Brenner, J.R. (1997b) Crystal growth of organohectorite clay as revealed by atomic force microscopy. *Langmuir*, **13**, 2895–2902.

Carrado, K.A., Xu, L., Gregory, D.M., Song, K., Seifert, S. and Botto, R.E. (2000) Crystallization of a layered silicate clay as monitored by small-angle X-ray scattering and NMR. *Chemistry of Materials*, **12**, 3052–3059.

Chapman, N.A. and Smellie, J.A.T. (1986) Introduction and summary of the workshop: natural analogues to the conditions around a final repository for high-level radioactive waste. *Chemical Geology*, **55**, 167–173.

Chung, K.H., Klenze, R., Park, K.K., Paviet-Hartmann, P. and Kim, J.I. (1998) A study of the surface sorption process of Cm(III) on silica by time-resolved laser fluorescence spectroscopy (I). *Radiochimica Acta*, **82**, 215–219.

Coppin, F., Berger, G., Bauer, A., Castet, S. and Loubet, M. (2002) Sorption of lanthanides on smectite and kaolinite. *Chemical Geology*, **182**, 57–68.

Farmer, V.C. (1974) *The Infrared Spectra of Minerals*. Monograph **4**, Mineralogical Society London.

Güven, N. (1988) Smectites. Pp. 497–560 in: *Hydrous Phyllosilicates (Exclusive of Micas)* (S.W. Bailey, editor). Reviews in Mineralogy, Vol. **19**, Mineralogical Society of America, Washington, D.C.

Hartman, P. (1987) Modern PBC theory. Pp. 209–253 in:

Morphology of Crystals (I. Sunagawa, editor). Terra Scientific Publishing Company, Tokyo.

Horrocks, W. De W. Jr. and Sudnick, D.R. (1979) Lanthanide ion probes of structure in biology. Laser-induced luminescence decay constants provide a direct measure of the number of metal-coordinated water molecules. *Journal of the American Chemical Society*, **101**, 334–340.

Hummel, W., Berner, U., Curti, E., Pearson, F.J. and Thoenen, T. (2002) Nagra/PSI chemical thermodynamic data base 01/01. *Radiochimica Acta*, **90**, 805–813.

Kimura, T. and Choppin, G.R. (1994) Luminescence study on determination of the hydration number of Cm(III). *Journal of Alloys and Compounds*, **213/214**, 313–317.

Luckscheiter, B. and Kienzler, B. (2001) Determination of sorption isotherms for Eu, Th, U and Am on the gel layer of corroded HLW glass. *Journal of Nuclear Materials*, **298**, 155–162.

Lukscheiter, B. and Nesovic, M. (1996) *Langzeitsicherheit der Endlagerung radioaktiver Abfälle: Entwicklung und Charakterisierung eines Glasproduktes für den HAWC der WAK, Forschungszentrum Karlsruhe (Long-term safety of the ultimate disposal of radioactive wastes. Development and characterization of a glass product for the HAWC of the WAK)*. Wissenschaftliche Berichte – Forschungszentrum Karlsruhe, FZKA 5825, pp. 1–130.

Madejová, J. and Komadel, P. (2001) Baseline studies of The Clay Minerals Society source clays: infrared methods. *Clays and Clay Minerals*, **49**, 410–432.

Malakul, P., Srinivasan, K.R. and Wang, H.Y. (1998) Metal adsorption and desorption characteristics of surfactant-modified clay complexes. *Industrial & Engineering Chemistry Research*, **37**, 4296–4301.

Mallants, D., Marivoet, J. and Sillen, X. (2001) Performance assessment of the disposal of vitrified high-level waste in a clay layer. *Journal of Nuclear Materials*, **298**, 125–135.

Maza-Rodriguez, J., Olivera-Pastor, P., Bruque, S. and Jimenez-Lopez, A. (1992) Exchange selectivity of lanthanide ions in montmorillonite. *Clay Minerals*, **27**, 81–89.

Meunier, A., Velde, B. and Griffault, L. (1998) The reactivity of bentonites: a review. An application to clay barrier stability for nuclear waste storage. *Clay Minerals*, **33**, 187–196.

Miller, S.E., Heath, G.R., Gonzalez, R.D. (1982) Effects of temperature on the sorption of lanthanides by montmorillonite. *Clays and Clay Minerals*, **30**, 111–122.

Miller, S.E., Heath, G.R. and Gonzalez, R.D. (1983) Effect of pressure on the sorption of Yb by montmorillonite. *Clays and Clay Minerals*, **31**, 17–21.

Moore, D.M. and Reynolds, R.C., Jr. (1997) *X-ray Diffraction and the Identification and Analysis of Clay minerals*. Oxford University Press, Oxford, New York.

Parkhurst, D.L. and Appelo C.A.J. (1999) User's guide to PHREEQC (version 2) – A computer program for speciation, batch-reaction, one-dimensional transport and inverse geochemical calculations. US Geological Survey.

Rochelle, C.A., Bateman, K., MacGregor, R., Pearce, J.M., Savage, D. and Wetton, P.D. (1996) *Experimental determination of chlorite dissolution rates*. Materials Research Society Symposium.

Shannon, R.D. and Prewitt, C.T. (1969) Effective ionic radii in oxides and fluorides. *Acta Crystallographica, Section B: Structural Crystallography and Crystal Chemistry*, **B25**, 925–946.

Stumpf, T., Bauer, A., Coppin, F. and Kim, J.I. (2001) Time-resolved laser fluorescence spectroscopy study of the sorption of Cm(III) onto smectite and kaolinite. *Environmental Science & Technology*, **35**, 3691–3694.

Stumpf, T., Bauer, A., Coppin, F., Fanghanel, T. and Kim, J.I. (2002) Inner-sphere, outer-sphere and ternary surface complexes: a TRLFS study of the sorption process of Eu(III) onto smectite and kaolinite. *Radiochimica Acta*, **90**, 345–349.

Sunagawa, I. (1987) Surface microtopography of crystal faces. Pp. 509–553 in: *Morphology of Crystals* (I. Sunagawa, editor). Terra Scientific Publishing, Tokyo.

Takahashi, Y., Kimura, T., Kato, Y., Minai, Y. and Tominaga, T. (1998) Characterization of Eu(III) species sorbed on silica and montmorillonite by laser-induced fluorescence spectroscopy. *Radiochimica Acta*, **82**, 227–232.

Velde, B. (1995) *Origin and Mineralogy of Clays.* Springer-Verlag, Berlin, Heidelberg.

Vidal, O., Magonthier, M.-C., Joanny, V. and Creach, M. (1995) Partitioning of La between solid and solution during the aging of Si-Al-Fe-La-Ca gels under simulated near-field conditions of nuclear waste disposal. *Applied Geochemistry*, **10**, 269–284.

Zimmer, P., Bohnert, E., Bosbach, D., Kim, J.I. and Althaus, E. (2002) Formation of secondary phases after long-term corrosion of simulated HLW glass in brine solutions at 190ºC. *Radiochimica Acta*, **90**, 529–535.

Zwicky, H.U., Grambow, B., Magrabi, C., Aerne, E.T., Bradley, R., Barnes, B., Graber, T., Mohos, M. and Werme, L.O. (1989) Corrosion behavior of British Magnox waste glass in pure water. *Materials Research Society Symposium Proceedings*, **127** (*Scientific Basis for Nuclear Waste Management*, **12**), 129–136.

(*Received 10 August 2004; revised 7 October 2005; Ms. 951; A.E. James E. Amonette*)